BUCKLING OF CYLINDRICAL COMPOSITE SHELLS UNDER DEFORMATION-RELATED LOADS BY USING FINITE STRIP METHOD

Arman Amini
Safir-E-Andisheh Language Academy, Iran

Abstract

Current advances in today's industries increasingly expand the need for using composite materials in order to achieve desirable characteristics. Regarding the important role these materials play in engineering sciences, conducting precise analysis on such composites is admitted to be of great significance. One of the greatest weaknesses of these composites is their Shear Strength; hence, since the shear deformation has been ignored in the Classic Theory, the First Order Shear Theory has been adapted in the present paper. Deformation-related loads are loads in line with the loads resulted from deformation process which are usually being considered constant to facilitate load direction analyses. Shell materials have been set to be layered composites and the calculation method is of semi-analytical type. Displacement functions are defined as the combination of Fourier series in the perimeter dimension of shell and polynomial functions in the length dimension of shell. Results gathered from the proposed software for buckling of cylindrical shells have been compared with results from other references and also with those from ABAQUS finite element software suite.

Keywords: Cylindrical shells, finite strip method, First Order Shear Theory, buckling, deformation-related loads

Introduction

Combination of highly resistant fibers with modules of high elasticity at microscopic and macroscopic scales produces composites. Having high resistance, high stiffness-weight ratio, high damping ratio and low coefficient of thermal expansion, composites are quite useful in engineering industries for manufacturing different types of shells, cylindrical shells in particular. Considering the important role these materials play in engineering sciences, conducting precise analysis on such composites is admitted to be of great significance; hence, a great body of literature has been dedicated to this field. Anastasiadis and Simitses {1} have calculated the buckling of

cylindrical composite shells under the axial pressure by using the classic theory, First Order Shear Theory and next order shear theory for the radius, different thicknesses and different layering of cylindrical shells. They have used semi-analytical method for calculating the buckling load. Longanthan and Chang {2} have studied shell sustainability by considering the pressure stiffness. In this study, they have used Kuwitter equation to calculate the virtual work resulted from reformation-related stress and Sanderz's modified theory to calculate strains. Park and Kim have surveyed the sustainability of cylindrical shells under reformation-related axial loading. They have applied the strain energy equation to calculate tangential stiffness and have used virtual load to calculate geometrical stiffness and pressure stiffness. In their study, Subbiah and Natarajan {4} have studied nonlinear analysis of rotating composite shells by considering the existence of great deformations under axial and lateral stresses and existence of deformation-related lateral stress. Having used Fourier expansions in perimeter dimension and Lagrange elements in length dimension, Santos and Reddy {5} have calculated the buckling load and the free vibration of shells by using the semi-analytical method. Ovesy and Fazilati {6} have adapted finite strip method to analyze linear buckling and buckling of composite plates and shells. Wang and Dawe {7} have surveyed the buckling of composite shell structures through calculating the special value by suing finite strip method. They have used first order shear theory to calculate buckling load in different layering types and bearings.

In the present paper, the effect of considering pressure stiffness matrix of cylindrical composite shells has been studied. In order to calculate the buckling load, the finite strip semi-analytical method containing dual groups Lagrange elements in length dimension and closed strips in perimeter dimension was adapted. Due to the significance of shear deformation in composite materials, this paper used first order shear theory to conducting analyses and Sanderz's theory for Strain-displacement equations. The present paper has used virtual load method to calculate stiffness matrixes and special value method to calculate buckling load. Results for buckling load calculations at different thicknesses and lengths have been compared with those from other references and also with those from ABAQUS finite element software suite.

Theory and Derivation of Equations

A circle-section cylindrical shell with middle section curving radius of R, thickness of h and length of L is supposed. Cylindrical shells are consisted of homogeneous layers which are completely connected to each other. Coordinates system and and geometrical specifications are shown in

figure 1. Components of coordination system are (S, Θ, Z). The range of S axis is ($0 \le S \le L$), range of Θ perimeter angle is ($0 \le \Theta \le 2\pi$) and Z thickness line is ($-h/2 \le Z \le h/2$)

. Deformations in s, Θ, Z are u, v, w and rotations in Θ, s are $ß_{s \text{ and }} ß_{\Theta}$ respectively.

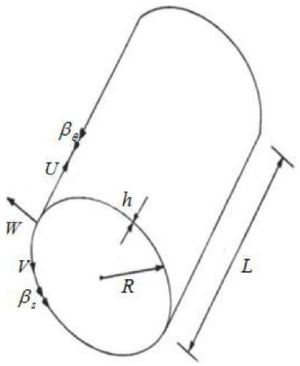

Fig. 1: Geometrical specifications and axes of coordinates of the shell

By considering first order shear theory, desired point displacement of the shell is such as Equation 1:

$$\begin{cases} \overline{U}(s,\theta,z) = U(s,\theta) + Z * \beta_s(s,\theta) \\ \overline{V}(s,\theta,z) = V(s,\theta) + Z * \beta_\theta(s,\theta) \\ \overline{W}(s,\theta,z) = W(s,\theta) \end{cases} \quad (1)$$

Buckling load is λ and buckling load-applied load ratio is q. After solving equation no.1, special value of equation 2 can appears:

$$\left| K^n - \lambda_{cr}\left(K_G^n + K_P^n\right) \right| = 0 \quad (2)$$

In Equation 2, K is tangential stiffness matrix, K_G is geometrical stiffness matrix and K_P is the matrix of pressure stiffness on the harmonic of n. The smallest value of λ is called λ_{cr} and its counterpart load is called buckling load ($q_{cr} = \lambda_{crq}$).

Geometrical and Tangential stiffness matrixes

Tangential stiffness matrix is calculated from the equation of virtual load for internal forces and anchors and their counterpart strains and through equation 3 as follows:

$$\delta W_{\text{int}} = \int_s \int_\theta \left(N_{ss}\delta\varepsilon_{ss}^{\ l} + N_{\theta\theta}\delta\varepsilon_{\theta\theta}^{\ l} + N_{s\theta}\delta\gamma_{s\theta}^{\ l} + M_{ss}\delta k_{ss}^{\ l} + M_{\theta\theta}\delta k_{\theta\theta}^{\ l} + M_{s\theta}\delta k_{s\theta}^{\ l} + Q_{ss}\delta\gamma_{ss}^{\ l} + Q_{\theta\theta}\delta\gamma_{\theta\theta}^{\ l} \right) R\, d\theta\, ds \quad (3)$$

In Equation 3, ε is the strain vector:

$$\varepsilon^T = \{\varepsilon_s \quad \varepsilon_\theta \quad \varepsilon_{s\theta} \quad k_s \quad k_\theta \quad k_{s\theta} \quad \gamma_s \quad \gamma_\theta\} \quad (4)$$

$\varepsilon_{s\Theta}$, ε_{Θ} and ε_s are the middle section strains, $K_{s\Theta}$, K_{Θ} and K_s are the middle section curvature and Υs and $\Upsilon\Theta$ are the shear strain in thickness.

Linear strain-displacement equations (based on Sanderz's theory) are as follows:

$$\varepsilon_s=\frac{\partial u}{\partial s}\qquad \varepsilon_\theta=\frac{1}{R}\frac{\partial v}{\partial \theta}+\frac{w}{R}\qquad \gamma_{s\theta}=\frac{\partial v}{\partial s}+\frac{1}{R}\frac{\partial u}{\partial \theta}\qquad \gamma_s=\beta_s+\frac{\partial w}{\partial s}\qquad k_s=\frac{\partial \beta_s}{\partial s}\qquad k_\theta=\frac{1}{R}\frac{\partial \beta_\theta}{\partial \theta}$$
$$\gamma_\theta=\beta_\theta+\frac{1}{R}\frac{\partial w}{\partial \theta}-\frac{v}{R}\qquad k_{s\theta}=\frac{\partial \beta_\theta}{\partial s}+\frac{1}{R}\frac{\partial \beta_s}{\partial \theta}+\frac{\partial v}{2R\partial s}+\frac{1}{2R}\frac{\partial u}{\partial \theta} \tag{5}$$

Nonlinear strain-displacement equations (based on Sanderz's theory) are as follows:

$$\varepsilon_s^{nl}=\frac{1}{2}\left(\frac{\partial w}{\partial s}\right)^2+\frac{1}{2}\left(\frac{\partial u}{\partial s}\right)^2+\frac{1}{2}\left(\frac{\partial v}{\partial s}\right)^2\qquad \varepsilon_\theta^{nl}=\frac{1}{2R^2}\left(\frac{\partial w}{\partial \theta}-v\right)^2+\frac{1}{2R^2}\left(\frac{\partial v}{\partial \theta}+w\right)^2+\frac{1}{2R^2}\left(\frac{\partial u}{\partial \theta}\right)^2$$
$$\varepsilon_{s\theta}^{nl}=\frac{1}{R}\frac{\partial w}{\partial s}\left(\frac{\partial w}{\partial \theta}-v\right)+\frac{1}{R}\frac{\partial v}{\partial s}\left(\frac{\partial v}{\partial \theta}+w\right)+\frac{1}{R}\frac{\partial u}{\partial s}\frac{\partial u}{\partial \theta} \tag{6}$$

In Equation3, $N\Theta$ and Ns are normal shell force in length unit, $Ns\Theta$ is the shear force on length unit, Ms and $M\Theta$ are curving anchors on the length unit, $Ms\Theta$ is the torsion anchor on length unit and Qs and $Q\Theta$ are shear force along thickness on length unit.

The relationship between forces and strains is formed by matrix of reduced stiffness of composite shell (equation 7).

$$\begin{Bmatrix} N_s\\ N_\theta\\ N_{s\theta}\\ M_s\\ M_\theta\\ M_{s\theta}\\ Q_s\\ Q_\theta \end{Bmatrix}=\begin{bmatrix} A_{11} & A_{12} & A_{16} & B_{11} & B_{12} & B_{16} & 0 & 0\\ A_{12} & A_{22} & A_{26} & B_{12} & B_{22} & B_{26} & 0 & 0\\ A_{16} & A_{26} & A_{66} & B_{16} & B_{26} & B_{66} & 0 & 0\\ B_{11} & B_{12} & B_{16} & D_{11} & D_{12} & D_{16} & 0 & 0\\ B_{12} & B_{22} & B_{26} & D_{12} & D_{22} & D_{26} & 0 & 0\\ B_{16} & B_{26} & B_{66} & D_{16} & D_{26} & D_{66} & 0 & 0\\ 0 & 0 & 0 & 0 & 0 & 0 & A_{44} & A_{45}\\ 0 & 0 & 0 & 0 & 0 & 0 & A_{45} & A_{55} \end{bmatrix}*\begin{Bmatrix} \varepsilon_s\\ \varepsilon_\theta\\ \gamma_{s\theta}\\ k_s\\ k_\theta\\ k_{s\theta}\\ \gamma_s\\ \gamma_\theta \end{Bmatrix} \tag{7}$$

In Equation 7, Dij, Bij and Aij are tensile stiffness, torsion stiffness and bending stiffness of multilayer composite shell which are calculated through Equation 8 as follows:

$$\begin{cases} \left(A_{ij},B_{ij},D_{ij}\right)=\int_h\left(1,Z,Z^2\right)\overline{Q_{ij}}dZ & \text{i , j=1,2,6}\\ A_{ij}=\int_h\left(Z\right)\overline{Q_{ij}}dZ & \text{i , j=4,5} \end{cases} \tag{8}$$

Transformed stiffness matrix is calculated by Equation 9:

$$\overline{Q_{ij}}=T^{-1}Q_{ij}T \tag{9}$$

In Equation 9, Qij is stiffness matrix of each layer and T is the transformation matrix of each layer.

Displacement terms of w, v, u, ßϴ and ßs are defined by using Fourier expansion in perimeter dimension. The adapted expansion for harmonic n is as Equation 10:

$$\begin{cases} u(s,\theta)=\left(u^{o}(s)+\sum_{i=1}^{NH}\left[u^{cn}(s)\cos(kn\theta)+u^{sn}(s)\sin(kn\theta)\right]\right) \\ v(s,\theta)=\left(v^{o}(s)+\sum_{i=1}^{NH}\left[v^{cn}(s)\cos(kn\theta)+v^{sn}(s)\sin(kn\theta)\right]\right) \\ w(s,\theta)=\left(w^{o}(s)+\sum_{i=1}^{NH}\left[w^{cn}(s)\cos(kn\theta)+w^{sn}(s)\sin(kn\theta)\right]\right) \\ \beta_{\theta}(s,\theta)=\left(\beta_{\theta}^{o}(s)+\sum_{i=1}^{NH}\left[\beta_{\theta}^{cn}(s)\cos(kn\theta)+\beta_{\theta}^{sn}(s)\sin(kn\theta)\right]\right) \\ \beta_{s}(s,\theta)=\left(\beta_{s}^{o}(s)+\sum_{i=1}^{NH}\left[\beta_{s}^{cn}(s)\cos(kn\theta)+\beta_{s}^{sn}(s)\sin(kn\theta)\right]\right) \end{cases} \tag{10}$$

Matrix of geometrical stiffness is calculated by the equation of virtual work for shell forces and their counterpart nonlinear strains (equation 11):

$$\delta W_{\text{int}}=\int_{s}\int_{\theta}\left(N_{ss}\delta\varepsilon_{ss}^{nl}+N_{\theta\theta}\delta\varepsilon_{\theta\theta}^{nl}+N_{s\theta}\delta\gamma_{s\theta}^{nl}\right)Rd\theta ds \tag{11}$$

Pressure stiffness matrix

To calculate the pressure stiffness matrix, the followings should be taken into account:

1. The load applied to the shell should be vertical to shell before and after the occurrence of deformation.
2. The load applied should be upon the middle fiber in the shell.
3. Deformation of shell is considered to be included in small deformations range
4. The load value is considered constant at the moment of deformation

Point displacement vector from shell in general coordinates is defined as Equation 12:

$$\vec{U}=u\vec{t}+w\vec{n}+v\vec{n}_{\theta}=u\left(\vec{k}\right)+w\left(\cos\theta\vec{i}+\sin\theta\vec{j}\right)+v\left(-\sin\theta\vec{i}+\cos\theta\vec{j}\right) \tag{12}$$

Point vector from middle fiber after deformation is calculated by Equation 13:

$$\vec{R}^{*}=\vec{R}+\vec{U} \tag{13}$$

In equation13, vector R is the initial point vector started from middle fiber before deformation.

Virtual work resulted from live load (deformation-related stress (load)) is defined by Equation 14:

$$\delta W_{no}^{ql} = \int\int \left(P^l dS^* \vec{n}^* \right) . \delta \vec{U} \tag{14}$$

In Equation 14, dS* is the area of the deformed element, n* is the normal vector on the deformed element surface and P is the live load (stress). Live load can be a function of s or Θ in first coordinates of the element. δU is the virtual displacement (Equation 15):

$$\delta \vec{U} = \delta u \vec{t} + \delta w \vec{n} + \delta v \vec{n}_\theta = \delta u \left(\vec{k} \right) + \delta w \left(\cos\theta \vec{i} + \sin\theta \vec{j} \right) + \delta v \left(-\sin\theta \vec{i} + \cos\theta \vec{j} \right) \tag{15}$$

By using vector analysis for the area and the normal vector of deformed element, Equation 16 stands as follows:

$$dS^* \vec{n}^* = \frac{\partial \vec{R}^*}{\partial \theta} d\theta \times \frac{\partial \vec{R}^*}{\partial s} dS \tag{16}$$

By expanding Equations 14 and 16, using Integration by Parts method and performing necessary simplifications, external virtual work which is resulted from live load is calculated as Equation 17:

$$\delta W_{ext} = \left(-\delta \int\int \left(P^l \left(\frac{v^2}{2R} + \frac{w^2}{2R} + w \frac{\partial u}{\partial s} R + w \frac{\partial v}{\partial \theta} \right) \right) ds d\theta + \int_0^l P^l \left(w \delta v \frac{\partial z}{\partial s} \right)_0^{2\pi} ds + \int_0^{2\pi} P^l \left(w \delta u R \right)_0^l d\theta \right) \tag{17}$$

First, a static analysis to calculate existed pressures is performed by using tangential stiffness matrix for loading process of the present case. Geometrical stiffness matrix is then calculated by the use of results gathered from the first step. After that and by considering PS, buckling load is calculated by using the two previous matrixes and the matrix of pressure stiffness. Without considering PS, buckling load is calculated by using geometrical stiffness matrix, tangential stiffness matrix and Equation 2.
Precise integration in perimeter dimension and nominal integration with Gaussian method in length dimension have been used in the software which has been coded in MATLAB software suite to calculate buckling load.

Results

Example #1:

In this example, a both ends fixed cylindrical shell under uniform lateral pressure is being examined. Results have been calculated for length-radius ratio of L/R and thickness of h. Shell radius is R=190.5mm (Figure 3). Material specifications are as follows:

$$E_1 = 206.844 * 10^9 Pa \quad E_2 = 18.6159 * 10^9 Pa \quad G_{12} = G_{13} = 4.48162 * 10^9 Pa \quad G_{23} = 2.55107 * 10^9 Pa$$

$$\upsilon_{12} = 0.21$$

In the present paper, the difference between buckling load with PS and buckling load without PS is presented through μ. (Equation 18)

$$\mu(\%) = \left| \frac{q_{cr\,(without\ PS)} - q_{cr\,(with\ PS)}}{q_{cr\,(with\ PS)}} \right| * 100 \qquad (18)$$

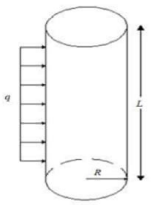

Figure 2: Cylindrical shell under lateral load

In present analysis, a dual-group element for each of 40 strips in length dimension has been used.

Table 1.2: Buckling load (Pa) for layering {90/90/90}s.

H	L/R	n	Without-PS[8]	With-PS[8]	Present Without-PS	Present With-PS	μ(%)
3.175	1	5	3.42E+06	3.30E+06	3.40E+06	3.28E+06	3.6
3.175	2	4	1.95E+06	1.84E+06	1.94E+06	1.83E+06	6.0
3.175	5	3	9.41E+05	8.44E+05	9.40E+05	8.41E+05	11.7
6.35	1	5	1.85E+07	1.80E+07	1.84E+07	1.75E+07	5.4
6.35	2	3	1.11E+07	1.00E+07	1.10E+07	9.89E+06	10.9
6.35	5	3	5.99E+06	5.39E+06	5.98E+06	5.35E+06	11.7
12.7	1	4	9.23E+07	8.87E+07	9.13E+07	8.65E+07	5.6
12.7	2	3	5.26E+07	4.82E+07	5.20E+07	4.69E+07	10.8
12.7	5	2	2.83E+07	2.22E+07	2.79E+07	2.16E+07	29.4

Table 1.2: Buckling load (Pa) for layering {0/90/0}s.

H	L/R	n	Without-PS[8]	With-PS[8]	Present Without-PS	Present With-PS	μ(%)
3.175	1	7	2.283E+06	2.241E+06	2.283E+06	2.239E+06	2.0
3.175	2	5	1.086E+06	1.044E+06	1.085E+06	1.043E+06	4.0
3.175	5	4	5.321E+05	4.997E+05	5.320E+05	4.992E+05	6.6
6.35	1	6	1.488E+07	1.452E+01	1.488E+07	1.448E+07	2.7
6.35	2	4	6.175E+06	5.820E+06	6.163E+06	5.796E+06	6.3
6.35	5	3	2.794E+06	2.496E+06	2.790E+06	2.487E+06	12.2
12.7	1	5	8.822E+07	8.635E+07	8.825E+07	8.567E+07	3.0
12.7	2	4	3.472E+07	3.292E+07	3.466E+07	3.258E+07	6.4
12.7	5	3	1.629E+07	1.465E+07	1.627E+07	1.450E+07	12.2

As it can be seen in table 1, results for buckling load have acceptable precision compared with the paper involved in comparison. Difference in buckling load with Ps is due to the calculation method. In Reference No. 8, live load has been used since the Kuwitter's equation was adapted to calculate virtual work (Kuwitter's equation is based on changes of mass of the given element at the time of applying the load.).

Example #2:

In this example, the cylindrical shell is under hydrostatic pressure and has a simple bearing for layering {α/-α}. Shell radius is R=190.5mm and materials are the same as example #1.

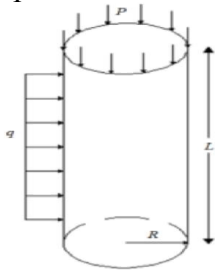

Figure 3: Cylindrical shell under hydrostatic pressure

In hydrostatic pressure, it is supposed that shell is at a deep depth in fluid and axial pressure is 2/R. Table 2 compares the results of analysis of ABAQUA software for thickness of 3.175mm and length-radius ratio of 5. In ABAQUA software, S8R shell element has been adapted; also, 40 strips in length dimension and reduced integration method have been used as well.

$$error(\%) = \frac{Abaqus - Code}{Abaqus} * 100$$

Table 2: Comparison of the results of proposed software with those of ABAQUS software suite

Lay-up	Code (without-PS) (Pa)	Abaqus (without-PS) (Pa)	%error
[5/-5]s	2.186E+05	2.197E+05	0.49
[10/-10]s	2.324E+05	2.334E+05	0.43
[15/-15]s	2.472E+05	2.481E+05	0.38
[20/-20]s	2.632E+05	2.641E+05	0.34
[25/-25]s	2.861E+05	2.870E+05	0.31
[30/-30]s	3.172E+05	3.176E+05	0.10
[35/-35]s	3.292E+05	3.295E+05	0.10
[40/-40]s	3.661E+05	3.665E+05	0.11
[45/-45]s	4.257E+05	4.262E+05	0.11
[50/-50]s	4.733E+05	4.731E+05	-0.05
[55/-55]s	5.247E+05	5.244E+05	-0.05
[60/-60]s	5.907E+05	5.903E+05	-0.08
[65/-65]s	6.603E+05	6.596E+05	-0.11
[70/-70]s	7.252E+05	7.242E+05	-0.14
[75/-75]s	7.784E+05	7.772E+05	-0.15
[80/-80]s	8.130E+05	8.118E+05	-0.14
[85/-85]s	8.245E+05	8.236E+05	-0.12
[90/-90]s	8.232E+05	8.223E+05	-0.10

Regarding the data on table 2, it can be concluded that proposed software enjoys acceptable level of precision since the maximum error of results is 0.49%.

Figures 1-1 to 1-3 show the buckling loads for the following data: length-radius ratios of 5 and 10, 3 different thicknesses and existence or absence of PS.

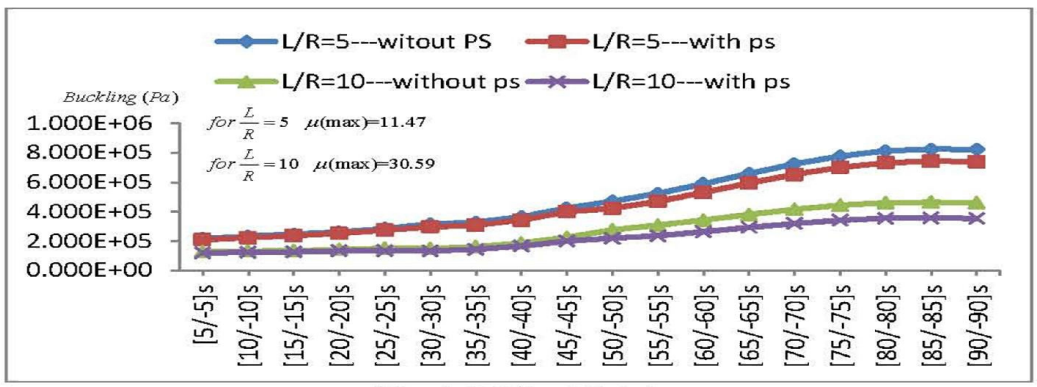

Figure 1-1: thickness of h=3.175mm

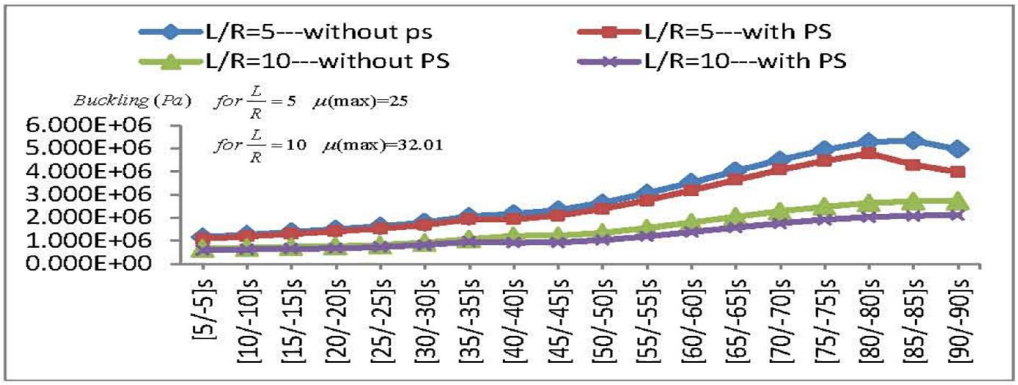

Figure 1-2: thickness of h=6.35mm

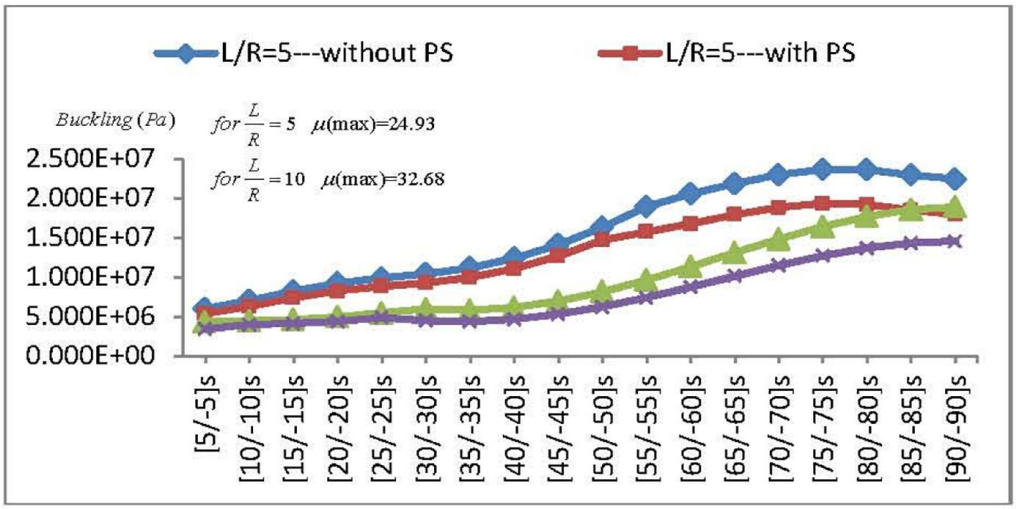

Figure 1-3: thickness of h=12.7mm

Diagram 1: comparison of buckling loads with and without PS

Considering figures 1-1 to 1-3 and Table 1, we come to this conclusion that considering PS can hugely decrease the buckling load. Also, the effect of live load will increase as thickness and length of thin plates do so. In addition, diagram 1 shows the effect of changing the layering angle on the effect of PS on buckling load; widening the layering angle from 0 to 90 degrees increases the effect of PS on buckling load.

On the other hand, reducing the modes of shell buckling will increase the effect of PS in decreasing buckling load. Diagram 2 shows the effect of reducing the number of harmonics for a shell with thickness of 3.175mm and length-radius ratio of 10. In the mentioned diagram, reducing the number of harmonics would increase the value of μ.

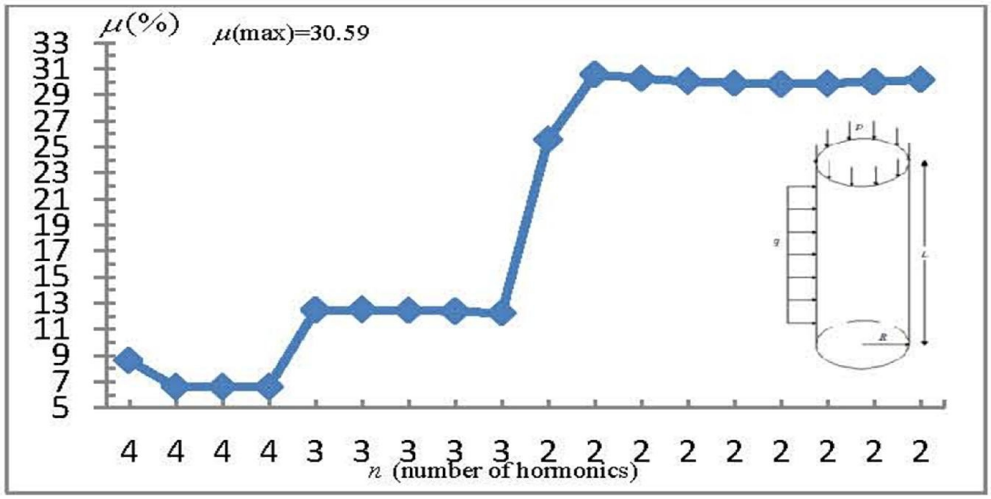

Diagram 2: the effect of buckling modes on the effect of PS matrix

Conclusion

The present paper has studied the effect of pressure stiffness (deformation-related pressure) on the value of buckling load by using finite strip method and Fourier expansions. Data on tables 1 and 2 show the precision and reliability of the proposed software; also, results reveal that considering a fixed direction for a load at the time of deformation will lead to some degree of uncertainty in calculating the final value. This issue is due to this fact that buckling load is smaller when the effect of live load is considered than the cases when this effect is not considered. In addition, it should be noted that considering the effect of live load will increase the design costs. Regarding the analyses conducted in this paper, it can be concluded that increasing thickness and length of shell increases the effect of pressure stiffness on decreasing the calculated value of buckling load. This butterfly effect shows the importance of considering live load in studying buckling load value.

Refrences

John S. Anastasiadis ,George J. Simitses,'' Buckling of pressure-loaded, long, shear deformable, cylindrical laminated shells'', J. *Composite Structures,* Vo.23,1993,pp.221-231

K. Longanthan, S.C. Chang, R.H. Gallagher,'' Finite element representation and pressure stiffness in shell stability analysis'', International journal for numerical methods in engineering ,Vo.14,1979,pp.1413-1429

Si- Hyoung Park, Ji-Hwan Kim,'' Dynamic stability of a stiff-edged cylindrical shell subjected to a follower force'', Computers and Structures, Vo.80,2002,pp.227-233

J. Subbiah, R. Natarajan,'' Stability analysis of ring stiffened shells of revolution, Computer and structures , VO.14,NO.5-6,1981,pp.479-490
Henrique Santos, Cristovao M. Mota Soares, Carlos A. Mota Soares, J.N. Reddy,'' A semi-analytical finite element model for the analysis of laminated 3D axisymmetric shell: bending, free vibration and buckling'', *J. Composite Structures*,Vo.71,2005,pp.273-281
H.R. Ovesy, J. Fazilati,'' Stability analysis of composite laminated plate and cylindrical shell structures using semi-analytical finite strip method'', J. Composite Structures ,Vo.89,2009,pp.467-474
Wang, S., Dawe, D.J., "Buckling of composite shell structures using the spline finit strip method, Composites", Vol.30, 1999, pp. 351-364.
Izzet U. Cagdas, Sarp Adali,'' Buckling of cross-ply cylindrical under hydrostatic pressure considering pressure stiffness'', Ocean Engineering,Vo. 38,2011,pp.559-569